

NONLINEAR COCHLEA DYNAMICS AND THE UPPER LIMIT OF THE HUMAN AUDITORY SYSTEM

Hamadiche Mahmoud
LMFA, CNRS 5509, Ecully, France

ABSTRACT

A nonlinear mathematical model is developed here to analyze the passive mechanism of the inner ear, the cochlea. A strong interaction between the flow in the scala vestibuli and in the scala tympani and the basilar membrane is allowed by the model. The resonance frequencies and resonance wave numbers of the cochlea are found by solving an eigenvalues problem resulting from a linear version of the model. In the nonlinear version of the model, it was possible to eliminate explicitly the potential flow from the dynamic equation in order to obtain an integro-differential equation involving only the displacement of the basilar membrane. It is shown that the cochlea has a discrete resonance frequencies and discrete resonance wave numbers. One of the sets of the resonance frequencies is a double resonance formed by the coalescence of two resonance wave numbers. It is also shown that the basilar membrane no longer moves if the stimulus frequency exceeds some critical value highlighting the existence of the upper limit of hearing. The relationship between the high roll-off frequency and the stiffness of the basilar membrane is established and is found to be a parabolic one. Moreover, the upper limit of hearing increases with the increase of Young's modulus of the basilar membrane. It is found that the amplitude of basilar membrane oscillation at low frequency stimuli is higher than its counterpart at high frequencies. The apex of the basilar membrane is more excited by low frequencies than its base. And conversely, the base is more excited by high frequencies than the apex, in spite of the fact that Young's modulus of the basilar membrane used in the model is constant

1. INTRODUCTION

The ear is a complex and very sensitive organ of the living body. One of the major tasks of the ear is to detect and analyze noises by transduction. The ear is divided into three different parts, the outer ear, the middle ear and the inner ear. In

this work we shall study the mechanical behavior of the inner ear (the cochlea). The cochlea is a spiral, hollow, conical chamber made of bone. Structures include the scala vestibuli (containing perilymph) lies superior to the cochlea duct and abuts the oval window. The scala tympani (containing perilymph), which lies inferior to the scala media and terminates at the round window. The scala media (containing endolymph) is the membranous cochlea duct containing the organ of Corti. The helicotrema is the location where the scala tympani and the scala vestibuli merge. Reissner's membrane separates the scala vestibuli from the scala media. The basilar membrane separates the scala media from the scala tympani. The Organ of Corti is a cellular layer on the basilar membrane. It is lined with sensory cells topped with hair-like structures called stereo cilia. Humans can hear sound waves with frequencies between 20Hz and 20,000 Hz. The three bones in the ear (malleus, incus, stapes) transfer the vibrations, induced by an incoming acoustic wave, to the cochlea. When the hair cells are excited by vibrations, a nerve impulse is generated in the auditory nerve. These impulses are then sent to the brain. The inner ear may behave actively and passively in response to an incoming acoustic wave and is even able to generate spontaneous otoacoustic emissions (see De Boer et al. 1999, 2006). Understanding the passive mechanism of the cochlea is a necessary step toward a full understanding of the cochlea mechanism. In this paper we shall focus only on the passive mechanics of the inner ear. Models of the cochlea have been suggested by many authors. For instance, Nobili and Mammano (1993) have developed a linear model based on the Green function technique. De Beor (2000) measured the mechanical response of guinea-pig cochlea to broad-band noise, after which the measured results were analyzed using a linear model established by the author herself. She found that the cochlea could have passive as well as active mechanisms. Norman Sieroka et al. (2006) extended the model proposed by De Beor (1999), with the articles

referenced in their bibliography, to include long and short-wave approximations. In these models, a linearized Euler equation was solved to account for the dynamics of the fluid. A spring-like model has been proposed to account for the dynamics of the basilar membrane. In those models, the fluid pressure to the membrane velocity ratio has been assumed to be equal to the membrane impedance and the resonance frequency of the cochlea all of which depends exponentially on the axis of the cochlea. The pressure in the fluid is obtained by solving Poisson's equation in a stationary domain, whereas the Fourier transform is performed in an axial direction, leading to the two widely-known long-and short-wave approximations. In our model the flow is potential but in a time dependent domain and the pressure is obtained by the unsteady Bernoulli equation. Therefore, the pressure is a nonlinear function of velocity, contrary to the commonly admitted linear pressure-velocity relationship in the cochlea models. In order to take account of pending moments and flexural moments applied by the flow to the basilar membrane, we shall describe the dynamics of the basilar membrane by an elastic plan-shell equation. The kinematic conditions, namely the continuity of the velocity field, at the interface between the fluid and the shell are held without approximation. In that way a strong interaction between the fluid flow and the basilar membrane is allowed without introducing an artificial impedance assumption. Thus, our formulation leads to a mathematical model which is, to our best knowledge, the only one able to predict the high roll-off frequency. In order to simplify the mathematical formulation of the mechanical behavior of the cochlea, we shall regard it as a plane channel instead of a spiraled conical chamber, in the way it is schematically depicted in figure 1. The basilar membrane, Reissner's membrane, the scala media and the organ of Corti are regarded as an elastic shell. The fluid in the scala vestibuli channel and scala timpani channel are assumed to be non-viscous and the flow is irrotational.

Resonance frequencies and resonance wave numbers

The linear basic equation is obtained in the following way: the non linear terms are neglected in the governing equations, the terms involving the membrane displacement are eliminated by cross differentiation, a potential flow difference $\Phi = \Phi_1 - \Phi_2$ is introduced, where Φ_1 and Φ_2

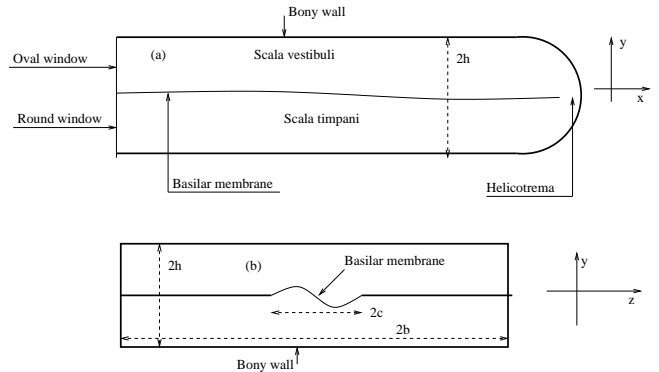


Figure 1: Diagram of the cochlea

are the potential flow in the scala vestibuli and in the scala timpani, which yields the following linear equation

$$\left[\frac{\partial^2}{\partial t^2} + D \left(\frac{\partial^2}{\partial x^2} - \beta^2 \right) \right] \frac{\partial^2 \phi}{\partial x^2} = 2\rho \frac{c}{b} \frac{\partial^2 \phi}{\partial t^2} \quad (1)$$

in this equation, ρ is the fluid mass density to solid mass density ratio. The dimensionless stiffness is

$$D = \frac{\epsilon^3 E}{12(1 - \nu^2)\rho_s h^4 \omega_0^2}, \quad \beta = \frac{\pi}{2c} \quad (2)$$

The boundary conditions associated with the precedent equation are

$$\begin{aligned} \frac{\partial \phi}{\partial x} = V, \quad \frac{\partial^2 \phi}{\partial x^2} = \frac{\partial^3 \phi}{\partial x^3} = 0; \quad x = 0 \\ \phi = 0, \quad \frac{\partial^2 \phi}{\partial x^2} = \frac{\partial^3 \phi}{\partial x^3} = 0; \quad x = L \end{aligned} \quad (3)$$

To find the resonance frequency and the resonance wave number, a solution is searched for in the form of a normal mode, namely

$$\phi = \tilde{\phi} e^{i\omega t + ikx} \quad (4)$$

substituting ϕ in equation (1) leads to the dispersion equation, so that

$$D(k^2 + \beta^2)^2 k^2 - (k^2 + 2\rho \frac{c}{b})\omega^2 = 0 \quad (5)$$

The frequency and the wave number in the dispersion equation are not arbitrary. Rather, the boundary condition leads to a set of discrete frequencies, ω_m , and discrete wave numbers, k_j^m , where $m = 1, 2, 3, \dots, \infty$ and $j = 1, 2, \dots, 6$. This is so because the dispersion equation has six roots for a given ω_m . Set (ω_m, k_j^m) is the resonance frequency and resonance wave numbers

of the cochlea. Figure 2 shows the discrete resonance numbers of the system. In this figure the resonance complex wave numbers are plotted versus the resonance frequencies. Figure 2a shows the real part and the imaginary part of two resonance complex wave numbers versus real frequencies. Those complex wave numbers become pure imaginary numbers at high frequency. At some frequency, those modes coalesce to form a second-order resonance; i. e., a more powerful resonance. The complex wave number where the coalescence takes place is marked by an arrow in the figure. In figure 2b two other complex resonance wave numbers are plotted versus the real frequencies. Those latter modes are the complex conjugate of former modes shown in figure 2a. Figure 2c Shows two pure imaginary wave numbers versus real frequencies. The real part of the complex number is the physical wave number and the imaginary part is the spatial amplification/damping rate. The frequency for which the coalescence occurs depends on the rheological parameters of the cochlea. In figure 2d, the variation of the double resonance frequency versus the membrane to fluid mass density ratio and for some values of aspect ratio β , are shown. For a thin basilar membrane the coalescence occurs at high frequencies. The group velocity of the wave propagating in the cochlea can be obtained from the dispersion relation, equation (5). That is, $V_g = -\frac{d\omega}{dk}$. It is found that, outside a small range of low frequency, the group velocity is an increasing function of frequency, ω , which is in qualitative agreement with the results obtained by solving the nonlinear equation found in the next section.

Nonlinear displacement equations

An integro-differential equation is established involving only the displacement of the basilar membrane to describe the dynamics of the cochlea. For it is shown that the two flow potentials Φ_1 and Φ_2 are such that

$$\Phi_1 = \int_x^L \left[\frac{1}{w(z) - \gamma} \int_0^z \frac{\partial w(\alpha)}{\partial t} d\alpha + \frac{\gamma V}{w(z) - \gamma} \right] dz$$

$$\Phi_2 = \int_x^L \left[\frac{1}{w(z) + \gamma} \int_0^z \frac{\partial w(\alpha)}{\partial t} d\alpha + \frac{\gamma V}{w(z) + \gamma} \right] dz$$

For simplification of terms we have introduced $\gamma = \frac{b\pi}{2c}$. Recall that the previous solution involves dimensionless variables where h is the unit

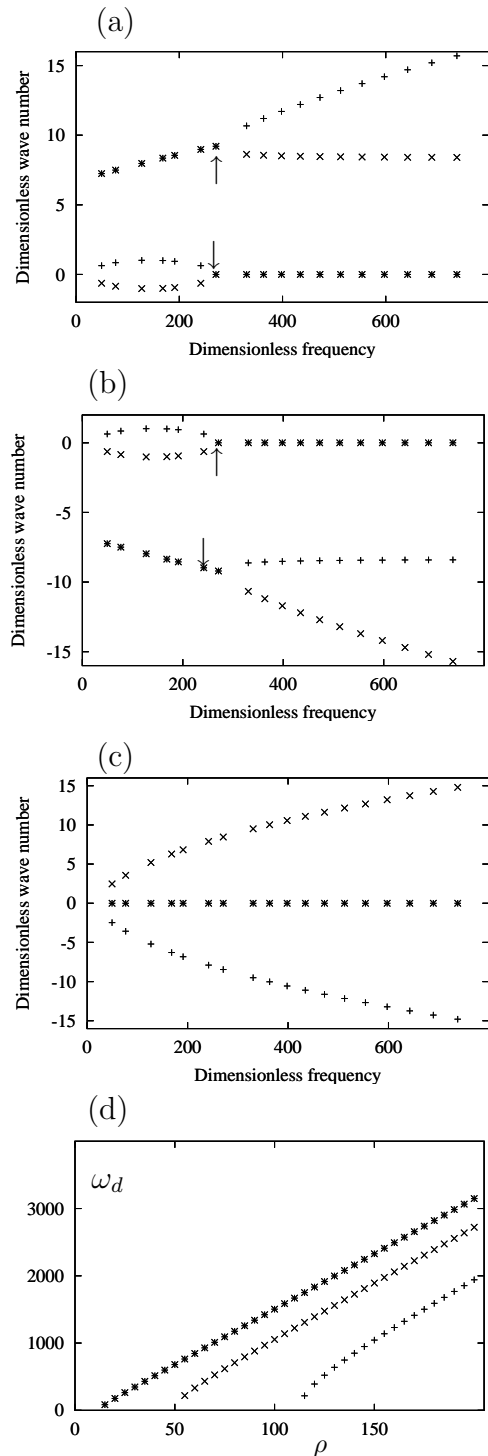


Figure 2: Sub-figures (a), (b) and (c) show the complex spatial eigenvalues versus the temporal eigenvalues; i. e., resonance wave numbers versus resonance frequencies. Sub-figure (d) shows the frequency where the coalescence of two spatial eigenvalues occurs, versus the mass density ratio ρ and for some β shape factor values. From the top curve to the bottom curve, $\beta = 20$, $\beta = 15$, $\beta = 10$.

of length. The arbitrary constants in both potentials are such that $\Phi_1 = \Phi_2 = 0$ at $x = L$. Using the Bernoulli equation to compute the pressure acting on the basilar membrane, which is viewed as a flat shell, the dynamic equation of the cochlea is written involving the only basilar membrane displacement. That is,

$$\begin{aligned} & \frac{\partial^2 w}{\partial t^2} + D \frac{\partial^4 w}{\partial x^4} - 2D\beta^2 \frac{\partial^2 w}{\partial x^2} + D\beta^4 w = \\ & \frac{\pi\rho}{2} \int_x^L \left[-\frac{\partial w(z)}{\partial t} \left(\frac{1}{(w(z) - \gamma)^2} - \frac{1}{(w(z) + \gamma)^2} \right) \right. \\ & \quad \left. \left(\int_0^z \frac{\partial w(\alpha)}{\partial t} d\alpha + \gamma V \right) \right] dz \\ & \frac{\pi\rho}{2} \int_x^L \left[\left(\frac{1}{w(z) - \gamma} - \frac{1}{w(z) + \gamma} \right) \right. \\ & \quad \left. \left(\int_0^z \frac{\partial^2 w(\alpha)}{\partial t^2} d\alpha + \gamma \frac{\partial V}{\partial t} \right) \right] dz \\ & + \frac{\pi\rho}{4} \left(\frac{1}{(w(x) - \gamma)^2} - \frac{1}{(w(x) + \gamma)^2} \right) \left[\right. \\ & \quad \left. \left(\int_0^x \frac{\partial w(\alpha)}{\partial t} d\alpha \right)^2 + (\gamma V)^2 \right] \quad (6) \end{aligned}$$

The boundary conditions associated to the precedent equation are

$$\begin{aligned} w = \frac{\partial w}{\partial x} = 0, & \quad x = 0 \\ w = \frac{\partial w}{\partial x} = 0, & \quad x = L \end{aligned} \quad (7)$$

Small displacement of the basilar membrane

The nonlinear equation (6) involves double integrations over the axial distance; consequently, it is time consuming in numerical simulation. Therefore, it is desirable to replace it by a more tractable equation without losing the precision desired in the results. We have at our disposal the fact that the membrane displacement is small in comparison with the size of the channels. Thus, the fraction is expanded involving w in equation (6) as follows

$$\begin{aligned} \left(\frac{1}{(w - \gamma)^2} - \frac{1}{(w + \gamma)^2} \right) & \approx \frac{4w}{\gamma^3} + O(w^2) \\ \left(\frac{1}{(w - \gamma)} - \frac{1}{(w + \gamma)} \right) & \approx -\frac{2}{\gamma} + O(w^2) \end{aligned} \quad (8)$$

then by neglecting all the terms involving a second or higher order in w , the shell equation be-

comes

$$\begin{aligned} & \frac{\partial^2 w}{\partial t^2} + D \frac{\partial^4 w}{\partial x^4} - 2D\beta^2 \frac{\partial^2 w}{\partial x^2} + D\beta^4 w = \\ & -\pi\rho(L - x) \frac{\partial V}{\partial t} + \frac{\pi\rho}{\gamma} w(x) V^2 \\ & - \frac{\pi\rho}{\gamma} \int_x^L \left(\int_0^z \frac{\partial^2 w(\alpha)}{\partial t^2} d\alpha \right) dz \quad (9) \end{aligned}$$

The boundary conditions, given by equation (7) remain unchanged. Equations (6) and (9) are solved by a spectral method. In this method only two boundary conditions are enforced; i.e., $w = 0$ at $x = 0$ and $x = L$. The numerical result may be improved by an expansion taking into account all the boundary conditions described by equation (7). However, because the basilar membrane is not perfectly rigid, no one really knows what the derivative of w at $x = 0$ and at $x = L$ is, therefore, it is preferable to have a tractable expansion and leave the mathematical rigor for another opportunity. Thus, a solution of equation (6)-(9) is searched for in the following series

$$w = \sum_{j=1}^N A_j(t) \sin\left(\frac{j\pi x}{L}\right) \quad (10)$$

Using the orthogonality of the trigonometric functions, equations (6) and (9) are transformed to a second order-system of differential equations and then solved by a fourth-order Runge-Kutta method. It has been found that the difference between the solution of equations (6) and (9) are less than 3% of the amplitude and insignificant difference in the phase for high frequencies, and an insignificant difference, in both amplitude and phase, has been found for low frequencies. From now on, equation (9) will be used to give insight into the membrane dynamics by an extensive computation.

Nonlinear results

In order to describe the reaction of the basilar membrane to an incoming monochromatic acoustic wave, the basilar membrane is considered at rest at $t = 0$ and the incoming acoustic wave forces the membrane of the oval window to move with a velocity $V = A \sin(\omega_w t)$, then, equation (9) is solved. The amplitude of the velocity of the membrane of the oval window, A , is connected to the pressure of the acoustic wave by the relation $p_a \approx \frac{1}{2} \rho_{air} A^2$ (stagnation pressure). The frequency ω_w is the frequency of the acoustic wave. From now on,

one can examine the following mean quantity $\langle w(x,t), w(x,t) \rangle = \int_0^L w(x,t)^2 dx$. That is the mean square membrane displacement. Plotting precedent quantity versus the external parameters of the system leads to a huge number of curves and figures. To avoid such a bad presentation only the maximum value reached by the precedent mean quantities will be plotted in a given time range. Thus, the dynamic equation is solved in the range $0 \leq t \leq t_{max}$, where t_{max} is large enough to allow the saturation of the amplitude of the displacement where a fully nonlinear regime is established. Then, the several obtained maximum versus the external parameters are plotted. Thus, for each value of the external parameters, the nonlinear system is solved until saturation, the maximum mean value is picked up and stored. The operation is repeated for the the desired value of the external parameters. The high roll-off frequency is an important characteristic of the cochlea because it determines the upper limit of the hearing. From a mechanical point of view, the high roll-off frequency occurs when the basilar membrane no longer moves under the action of a stimulus having a frequency above some critical value. In order to know if the upper hearing limit is a passive character of the cochlea or not, one can plot the maximum mean square displacement of the basilar membrane versus the stimulus frequency. The maximum mean square displacement is a positive quantity: it is clear that $\langle w, w \rangle = 0$ implies $w = 0$ and vice-versa. In figure 3, the maximum mean square displacement is plotted versus the stimulus frequency for some values of rheological parameter D . In order to obtain the curves in this figure, the nonlinear system has been solved more than 10^4 times, which is very difficult to do without the approximation done in the precedent section.

As long as the stimulus frequency is below the critical frequency, the maximum mean square displacement of the basilar membrane varies quasi periodically with the stimulus frequency, with a small increase in the period of oscillation with an increase in the stimulus frequency. When the stimulus frequency reaches the critical frequency, the maximum mean square displacement goes to zero; i. e., the basilar membrane stops moving. Therefore, the cochlea no longer catches the acoustic wave in perfect agreement with the observed daily behavior of the cochlea in living bodies. Figure 3 shows that the high roll-off frequency depends on the rheological parameters of the cochlea via D which involve thickness,

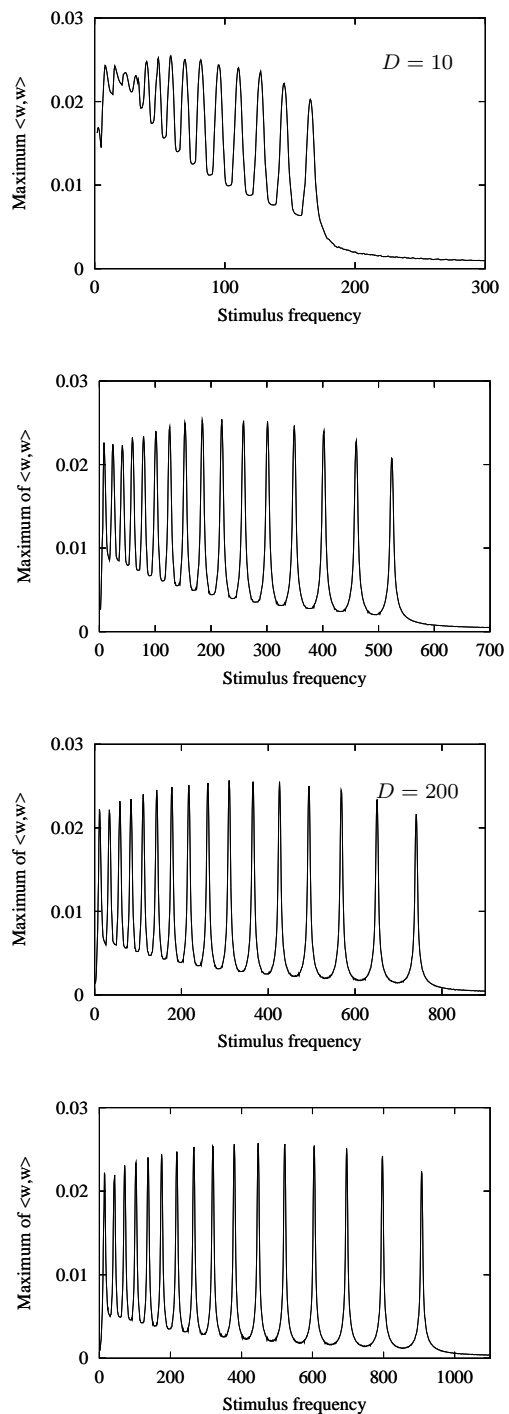


Figure 3: Mean displacement of the basilar membrane versus the stimulus frequencies, ω_w , for some values of D . The figures show that the mean displacement is no longer significant when the stimulus frequency exceeds the high roll-off frequency. (a): $D = 10$, (b): $D = 100$; (c): $D = 200$, (d): $D = 200$, $\rho = 35$, $\beta = 7$, $L = 6$, $A = 0.05$, the velocity of the oval window membrane $V = A \sin(\omega_w t)$.

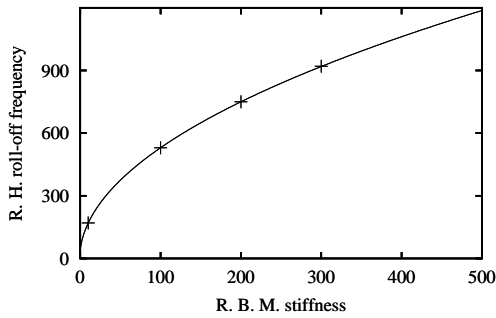


Figure 4: Relative high roll-off frequency versus relative stiffness of the basilar membrane

Young's modulus, Poisson's coefficient and the mass density of the basilar membrane the width, h , of scala vestibuli and scala timpani channels and the time Scale ω_0^{-1} , (see equation 2). The critical frequency of the upper hearing limit determined here is a dimensionless frequency. One has to multiply the dimensionless frequency by ω_0 to find the real limit. To compute ω_0 it is necessary to know the exact value of the rheological parameters. It is worthy to note that an inverse method may be used to compute the rheological parameters value. For if we know the high roll-off frequency we can compute ω_0 . The knowledge of which allows us to compute the value of one rheological parameter via equation (2) if all the other parameters are known. In figure 3 the maximum of the maximum of the mean displacement is observed. The maximum of the maximum occurs at some stimulus frequency for a given D . Increasing D shifts the maximum of the maximum toward the high frequency. Thus, the basilar membrane is more sensitive to some frequencies than others. This sensitivity depends on the rheological parameters which may indicate place to frequency dependence. Figure 4 shows the relative high roll-off frequency versus the dimensionless stiffness of the basilar membrane D . The frequency and the stiffness labeled + is obtained by extrapolation of the results shown in figure 3. Then the parabolic relation between the high roll-off frequency, ω_f , and the stiffness is postulated, namely

$$D = a\omega_r^2 + b\omega_r + c \quad (11)$$

then the collocation method is used to obtain the numerical values of the constants a , b and c . Thus, we found that $a = 0.0003527$, $b = 0.003135$, $c = -0.72492$. The curve in figure 4 fits those numerical values.

Acknowledgment

Thanks go to Dr. Christian J. Sumner for discussing the structures of cochlea with the author during at 6th annual meeting of Mathematics in Medicine Study Group in 2006 at Nottingham organized by The Physiological Flow Network.

2. REFERENCES

- [1] De Boer, E., Nuttall, A., L., 2000, Spontaneous basilar-membrane oscillation and coherent reflection. *JARO* 7:26-37, DOI: 10.1007/s10162-005-0020-9: 26-37.
- [2] De Boer, E., Nuttall, A., L., 2000, The mechanical waveform of the basilar membrane. III. Intensity effects. *J. Acoust. Soc. Am.*, **107**, (3): 1497-1507.
- [3] De Boer, E., Nuttall, A., L., 1999-INV-3, The inverse problem solved for a three-dimensional model of the cochlea. III. Brushing up the solution method. *J. Acoust. Soc. Am.*, **105**, (6): 3410-3420.
- [4] De Boer, E., 1997, Classical and no-classical model of the cochlea. *J. Acoust. Soc. Am.* **101**, (4): 2148-3728.
- [5] De Boer, E., 2000, The mechanical waveform of the basilar membrane. II. From data to models-and back. *J. Acoust. Soc. Am.*, **107**, (3): 1487-1496.
- [6] Nobili, R., Mammano, F. 1993, Biophysics of the cochlea: Linear approximation. *J. Acoust. Soc. Am.* **93**, (6): 3320-3332.
- [7] Sieroka, N., Dosch, H., G. and Rupp, A. 2006, Semirealistic models of the cochlea *J. Acoust. Soc. Am.* **120**, (1): 297-304.